# Modeling for cement materials exposed to external sulfate attack or delayed ettringite formation

**GU. Yushan[a], DANGLA. Patrick[b], FEN-CHONG. Teddy[c], OMIKRINE-METALSSI. Othman[d], MARTIN. Renaud-Pierre[e]**

a. IFSTTAR, yushan.gu@ifsttar.fr
b. Université Paris-Est, Laboratoire Navier UMR CNRS - Ecole des Ponts ParisTech - IFSTTAR, patrick.dangla@ifsttar.fr
c. IFSTTAR, teddy.fen-chong@ifsttar.fr
d. IFSTTAR, othman.omikrine-metalssi@ifsttar.fr
e. IFSTTAR, renaud-pierre.martin@ifsttar.fr

## Abstract :

*Sulfate attack is a well-known concrete degradation phenomenon induced by crystallization of ettringite, including external sulfate attack (ESA) and delayed ettringite formation (DEF). The differences between these two phenomenon are sources of sulfate ions and the positon of ettringite formed. For ESA, the sulfate ions diffuse from the exterior solution, and ettringite forms in the capillary pores. While for DEF, the sulfate ions are released from the CSH and contribute to ettringite crystalization in gel pores. A model, based on the homogeneous paste expansion and surface-controlled ettringite growth mechanism, is proposed to explain the both phenomenon in a uniform method. The crystallization pressure resulting from the supersaturated sulfate solution is believed to be the driving force for this mechanism. The ettringite forms first in the largest pores and then progresses to the smallest ones, no matter it is in capillary pores (ESA) or gel pores (DEF). When a crystal of ettringite nucleates on the pore wall, it will grow by consuming the excess of solute, and it will begin to exert stress on the solid matrix after it grows into contact with the opposite wall of the pore. The solid/crystal interface will rapidly reach equilibrium by exerting stress on the wall. Meanwhile the liquid/crystal interface will be out of equilibrium and will grow with a rate governed by an interface controlled growth mechanism until the crystal eventually sustains an isotropic stress state. Thus final stress state is obtained when the interfaces have reached a small enough radius of curvature as predicted by the Ostwald-Freundlich equation. The volume fraction of crystal, Sc(r), is introduced to describe the saturation degree of the crystal, which is related to the pore entry radius. In addition a poroelastic model is employed to predict the linear expansion of homogeneous samples exposed to sulfate attack. The comparison between the simulation and experimental results in literature has raised some issues that will be discussed.*

**Key words : sulfate attack, poromechanical model, surface-controlled ettringite growth mechanism**

# 1 Introduction

As is well-known, sulfate attack is a cause of concrete degradation. The most popular mechanism proposed in the literature is due to the crystallization of ettringite formed in the pores : capillary pores for External Sulfate Attack(ESA), and gel pores for Delayed Ettringite Formation (DEF) [1][2]. The expansion is believed to be caused by the homogeneous formation of ettringite, which leads to the swelling in the paste. The driving force for this mechanism is the pore pressure from the supersaturated sulfate solution. The porous materials is assumed saturated and the crystallization pressure of ettringite crystal is the basic mechanism responsible for the expansion of cementitious materials exposed to ESA or DEF. The external sulfate attack is described as the degradation both on the expansion and the decalcification of C-S-H, which is responsible for the binding capacity of the cement [3]. The loss of mechanical performance has been attributed to the formation of secondary sulfate-bearing phases from sulfate penetration from outside solutions. However, the source of sulfate ions for DEF is different. During the heat treatment, the primary ettringite is decomposed leading to more amount of sulphate and aluminate are trapped into C-S-H porosity. In the subsequent cooling storage, the temperature drop provokes the formation of secondary ettringite in the C-S-H gel from the calcium monosulphoaluminate in the C-S-H gel and absorbed sulphate, leading to the homogeneous expansion in the paste. A chemomechanical mathmatical model based on the diffusion-reaction approach, and several mechanisms for the reaction of calcium aluminates with sulfates to form expansive ettringite was proposed [4]. The crystal growth of ettringite is believed to be controlled by interface. If growth were under diffusion control, the crystal/liquid interface would be at the solubility limit, so no pressure could be tolerated [5]. The objective of this paper is to provide a poromechanical model founded on homogeneous paste expansion, surface-controlled crystal growth and other physicochemical properties both for ESA and DEF, despite of different sulfates sources and positions for crystal formation.

# 2 Model for crystallization-induced swelling

The expansion of a porous body, exposed to a supersaturated solution of a given crystal, is assumed to originate from the crystallization pressure exerted at the crystal/solid interface after crystal grows into contact with the wall of pore. The Coussy's theory [6] can be used to calculate the pressure caused by crystallization of salt. The linear strain $\varepsilon_x$, caused by crystallization pressure $P_c$, is approximately

$$\varepsilon_x \approx \frac{b}{3K} S_c P_c \tag{1}$$

In this equation $K$ is the bulk modulus of the porous body, $b$ is the Biot's coefficient and $S_{\mathrm{C}}$ is fraction of pore space saturated with the crystal. The crystallization pressure, $P_{\mathrm{C}}$, is the pressure needed to arrest growth in a supersaturated solution and is given by the Correns' equation [11] under the form :

$$P_{\mathrm{C}} = \frac{RT}{V_{\mathrm{C}}} \ln\left(\beta_C\right) \tag{2}$$

where $R$ is the ideal gas constant, $T$ is the temperature, $V_{\mathrm{C}}$ is the molar volume of the crystal, $\beta_{\mathrm{C}}$ is the saturation index of the crystal i.e. the ratio of the ion activity product and the solubility product.

Consider a cement-based material, whose pores are filled with supersaturated solution of ettringite. If a crystal of ettringite nucleates on the pore wall, it will grow by consuming the excess of solute, and it will begin to exert stress on the solid matrix after it grows into contact with the opposite wall of the

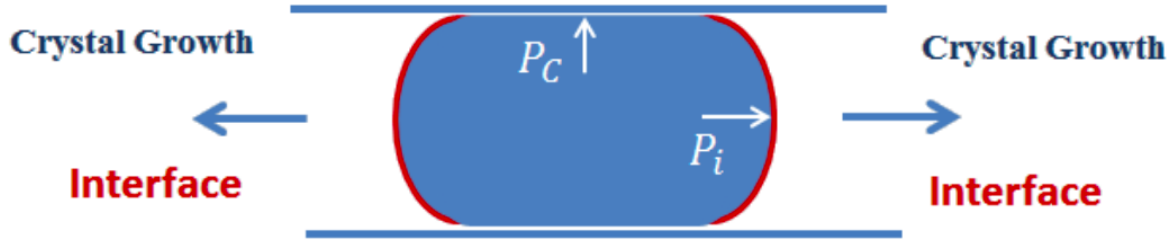


FIGURE 1 – Crystal Growth in one pore

pore. At the crystal/solid interface the crystal will rapidly stop growing and will then reach equilibrium by exerting stress on the wall according to Eq. (2). Meanwhile, the crystal/liquid interface will be out of equilibrium and will grow with a rate governed by an interface controlled growth mechanism [7], as described later on, until the crystal eventually sustains an isotropic stress state. The final isotropic stress state that the crystal will eventually sustain, is obtained when the crystal/liquid interface have reached a small enough radius of curvature as predicted by the Ostwald-Freundlich equation :

$$\frac{RT}{V_c}\ln(\beta_{\mathrm{AFt}}) = \frac{2\gamma_{CL}}{r} \tag{3}$$

where $\gamma_{CL}$ is the surface tension of AFt, $\gamma_{CL} = 0.1\mathrm{N/m}$ and $r$ is the mean radius of curvature of the interface at equilibrium.

Let us now model the crystal growth rate, and the crystal in our case is ettringite. It is assumed that the growth rate is governed by an interface controlled mechanism [7] given by

$$\frac{\mathrm{d}}{\mathrm{d}t}(S_{\mathrm{C}}) = a\left(1 - \exp\left(-\frac{\Delta G_r}{RT}\right)\right) \tag{4}$$

Where $a$ is a parameter which should be calibrated and $\Delta G_r$ is the reaction Gibbs energy of the crystal dissolution reaction, i.e $\Delta G_r = \sum_i \nu_i\mu_i - \mu_{\mathrm{C}}$ where the $\mu_i$ are the chemical potential of ions in solution, $\nu_i$ the stoichiometric coefficients and $\mu_{\mathrm{C}}$ the chemical potential of the solid crystal at the curved crystal/liquid interface which can be related to that of a flat interface through the Gibbs-Thomson equation, $\mu_{\mathrm{C}} = \mu_{\mathrm{C}}^{\infty} + 2\gamma_{\mathrm{CL}}V_{\mathrm{C}}/r$. It turns out that $\Delta G_r$ can be expressed as $\Delta G_r = RT\ln\left(\beta_{\mathrm{C}}/\beta_{\mathrm{C}}^{\mathrm{eq}}\right)$, so that a kinetic law for crystallization can be written as

$$\frac{\mathrm{d}}{\mathrm{d}t}(S_{\mathrm{C}}) = a\left(1 - \frac{\beta_{\mathrm{C}}^{\mathrm{eq}}}{\beta_{\mathrm{C}}}\right) \tag{5}$$

According to the literature, it is assumed that ettringite from ESA crystallizes in the biggest capillary pores and so the crystal saturation for ESA will be given by

$$S_c^{\mathrm{ESA}}(r) = 1 - S(r) \qquad r > r^{\mathrm{gel}} \tag{6}$$

On the other hand ettringite from DEF crystallizes in the biggest pores of the gel pore range and so

$$S_c^{\mathrm{DEF}}(r) = S(r^{\mathrm{gel}}) - S(r) \qquad r < r^{\mathrm{gel}} \tag{7}$$

# 3 Sensitivity analysis of parameters

Eq. (6) and Eq. ( 7) are solved by varying the parameters $a$ and $\beta_{\text{AFt}}$. As shown in Fig. (2), the kinetic constant $a$ has an effect on the rate only, both for capillary and gel pores. The crystal saturation with the higher kinetic constant reaches the final state faster. In return Fig. (3) shows that the ettringite saturation index contributes essentially to the final crystal saturation and has a restricted effect on the kinetics at the last moment before reaching equilibrium.

The higher saturation index forces ettringite to form in smaller pores, which in turn increases the crystal saturation and the time required to reach equilibrium. In this way the final expansion increases with the ettringite saturation index according to Eqs. (1) and (2) but the swelling kinetics in the early times only depends on the kinetic constant $a$. This latter observation enable us to calibrate the kinetic constant $a$ with experimental results during the early-time responses of samples. This is what we propose to do in the next sections.

# 4 Simulations

## 4.1 DEF simulations

Ettringite formation in hardened concrete after heat-treatment is often traced back to temperatures in concrete above the stability limit of ettringite. With rising temperature there is a drop in the thermodynamic stability of ettringite, which leads to the decomposition of the ettringite. Followed by a subsequent drop in temperature the monosulfate becomes metastable, so with sufficient water available ettringite can be formed again. This phase corresponds to a period of apparent inactivity with regard to the degradation at the macroscopic level, which is defined as latency period. However, this phase could not be presented in this proposed model, and a parameter $t_0$ is introduced, representing the duration of this period.
Firstly, with the fixed K and b, the saturation index of AFt is calibrated from the final expansion, as the $Pc$ and the maximum $Sc$ are related to $\beta_{AFt}$ only. Then, the kinetic constant $a$ is calibrated via the ratio $\varepsilon_i/\varepsilon_{max}$ from the experimental data in the literature, and $\varepsilon_{max}$ is the strain at maximum time.

### 4.1.1 First comparison

DEF experiments were performed in [1]. The calibration results for three sets of mortars bars [1] having different storage conditions are presented in this part. Expansion measurements were done on $16 \times 16 \times 160\text{mm}^3$ mortar bars with preheating : 20 °C for 4h, 90 °C for 12 h (with heating rates of 30-35 °C/h), cool naturally to 20 °C over about 5 h and in water afterwards. Two storage conditions were employed : 1) 20°C, and 2) 20°C 98 days and then 38°C. The modulus is adopted as 0.2GPa, and b is 0.99. The simulation results are presented in Fig. 4.

### 4.1.2 Second comparison

The effect of relative humidity on concrete expansion due to delayed ettringite formation is studied in [8]. The cylinders samples with 11 cm in diameter and 22 cm in height were made with siliceous aggregates and Portland cement CEM I 52.5N. All the samples were preheated : 20 °C for 2h, increase to 80°C with rate of 2.5°C/h, maintained at 80°C for 3 days, and decreased at a rate of -1 °C/h to 20°C. After the heating procedure, the samples were kept in different curing conditions. Two results are introduced

in this part, one is for 100% RH, and the other is stored at 91%RH firstly and then immersed in water from the age of 334 days. The simulation process is the same as above, and the results are showing as follows (Fig.5).

## 4.2 ESA simulations

From the experimental observation, the expansion for ESA samples is stopped at the accelerated deterioration phase. It is assumed that the observed expansion is just the beginning part of the swelling. A parameter $t_0$ is introduced representing the little swelling period.The calibration process is updated due to the lack of maximum swelling data. The growth rate of ettringite is assumed as the same as DEF, because the supersaturation of solution is the driving force for ettringite nucleation and growth. Specifically, the kinetic constant is adopted as $a_1 = 1 \times 10^{-8}$ in this part, which is calibrated above.

### 4.2.1 First comparison

A first set of ESA experiments were performed in [9]. Cement mortar samples were immersed in sulfate solution containing 4.3% magnesium sulfate and 2.5% sodium sulfate (by weight), with sulfate ion concentration of 0.573mol/L. Two kinds of mortars with different content in $C_3A$ (by weight) were used : 8.8% and 12%. The calibration results are shown in Fig. 6.

### 4.2.2 Second comparison

More experiments were performed in [10] where the effect of solution $p$H on expansion induced by sulfate attack is studied. In this experiment, mortar specimens made of 10% $C_3A$ Type I portland cement were immersed in 0.35 mol/L $Na_2SO_4$. In one case, the solution $p$H were allowed to vary, while in the other the $p$H was maintained at 6, 10 and 11.5. The comparisons are shown in Fig.7.

# 5 Discussion

1. The model based on the homogeneous paste expansion and surface-controlled ettringite growth mechanism is proposed for cement-based materials submitted to sulfate attack. It simulates the ettringite forming process, no matter it is in capillary pores (ESA) or gel pores in CSH (DEF). The poroelasticity theory is adopted to describe the swelling due to sulfate attack at this beginning stage. Two parameters are calibrated from the experimental results in literature : kinetic constant and saturation index of AFt. From the DEF calibration, the kinetic constants are consistently around $1 \times 10^{-8}$. According to the chemical reaction for ettringite formed in gel pores and boundary conditions for equilibrium saturation index of ettringite, the saturation index of ettringite could be determined by the saturation index of gypsum if the aluminate is buffered by hydrogarnet or monosulfate. As no gypsum is observed in the experimental phenomenon, the saturation index of gypsum should be less than 1, which means the saturation index of ettringite should be around $10^7$ for DEF and $10^{8.5}$ for ESA . The calibrated results for DEF is between $10^{7.5}$ to $10^{8.5}$ and $10^{8.2}$ to $10^{8.5}$ for ESA, which are acceptable.
2. The measured young modulus for mortar after leaching [12] is around 4.8 GPa, which is 10 times bigger than the value adopted in the model (0.1 – 0.6GPa). If the modulus is used as 5GPa in this model, the calibrated saturation index of AFt will be far beyond the reasonable range. For mortar sample, the strain at the maximum uniaxial tension stress is around $2 \times 10^{-4}$. It means the sample reaches to plastic

state before the ettringite accelerated growth phase. Therefore, a plasticity theory is considered to modify this model. In addition, the diffusing and leaching of the ions contribute to the saturation index of ettringite. Thus in the following step, a plasticity model considering the sulfate ions diffusion and alkali leaching will be proposed.

# Références

[1] Famy, Charlotte, Expansion of heat-cured mortars, Imperial College London (University of London), 1999.

[2] Johansen, Vagn and Thaulow, Niels and Skalny, Jan, Simultaneous presence of alkali—silica gel and ettringite in concrete, Advances in Cement Research, 1993, 5-17,23–29.

[3] Mehta, P, Sulfate attack on concrete–a critical review, Mater. Sci. Concr., IIIpp., 1992, 105.

[4] Tixier, RaphaÎl and Mobasher, Barzin, Modeling of damage in cement-based materials subjected to external sulfate attack. II : Comparison with experiments, Journal of materials in civil engineering, 2003, 15-4, 314–322.

[5] Scherer, George W ? Supersaturation in Porous Media.

[6] Coussy, Olivier, Deformation and stress from in-pore drying-induced crystallization of salt, Journal of the Mechanics and Physics of Solids, 2006, 54-8, 1517–1547.

[7] Knrpnrnrcr, R Jeuss, Crystal Growth from the Melt : A Review, Am Mineral, 1975, 60, 798–814.

[8] Al Shamaa, Mohamad and Lavaud, StÈphane and Divet, Loic and Nahas, Georges and Torrenti, Jean Michel, Influence of relative humidity on delayed ettringite formation, Cement and Concrete Composites, 2015, 58, 14–22.

[9] Ouyang, Chengsheng and Nanni, Antonio and Chang, Wen F, Internal and external sources of sulfate ions in Portland cement mortar : two types of chemical attack, Cement and Concrete Research, 1988, 18-5, 699–709.

[10] Brown, Paul Wencil, An evaluation of the sulfate resistance of cements in a controlled environment, Cement and Concrete Research, 1981, 11-5-6, 719–727.

[11] Correns, Carl W, Growth and dissolution of crystals under linear pressure, Discussions of the Faraday society 1949, 5, 267–271.

[12] Heukamp, Franz Hoyte, Chemomechanics of calcium leaching of cement-based materials at different scales : The role of CH-dissolution and CSH degradation on strength and durability performance of materials and structures, Massachusetts Institute of Technology, 2003.

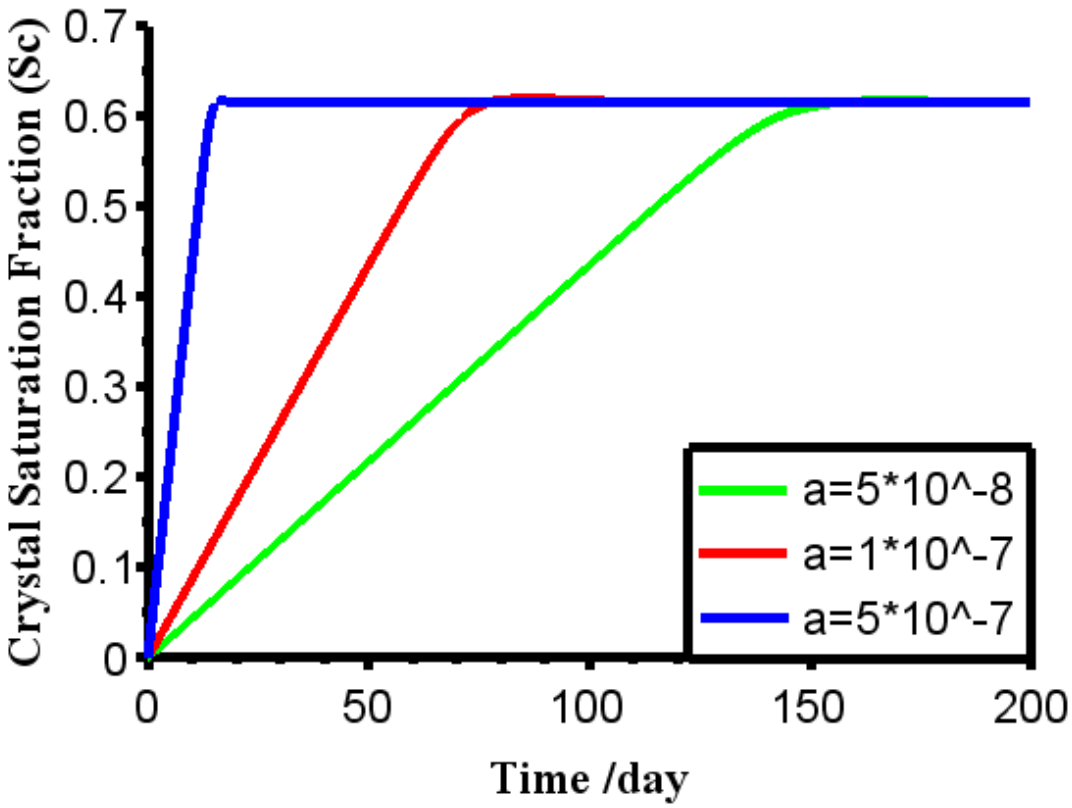


(a) in capillary pores $\beta_{\text{AFt}} = 10^5$

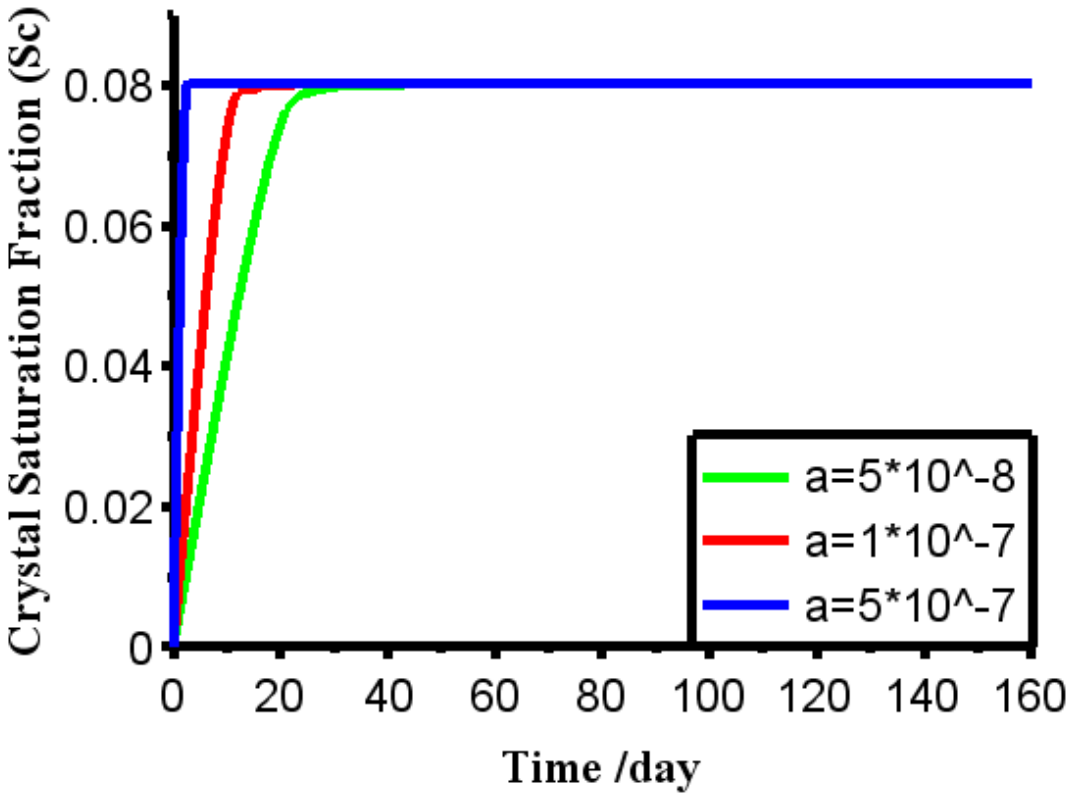


(b) in gel pores $\beta_{\text{AFt}} = 10^5$

FIGURE 2 – Effect of the kinetic constant on the crystal saturation

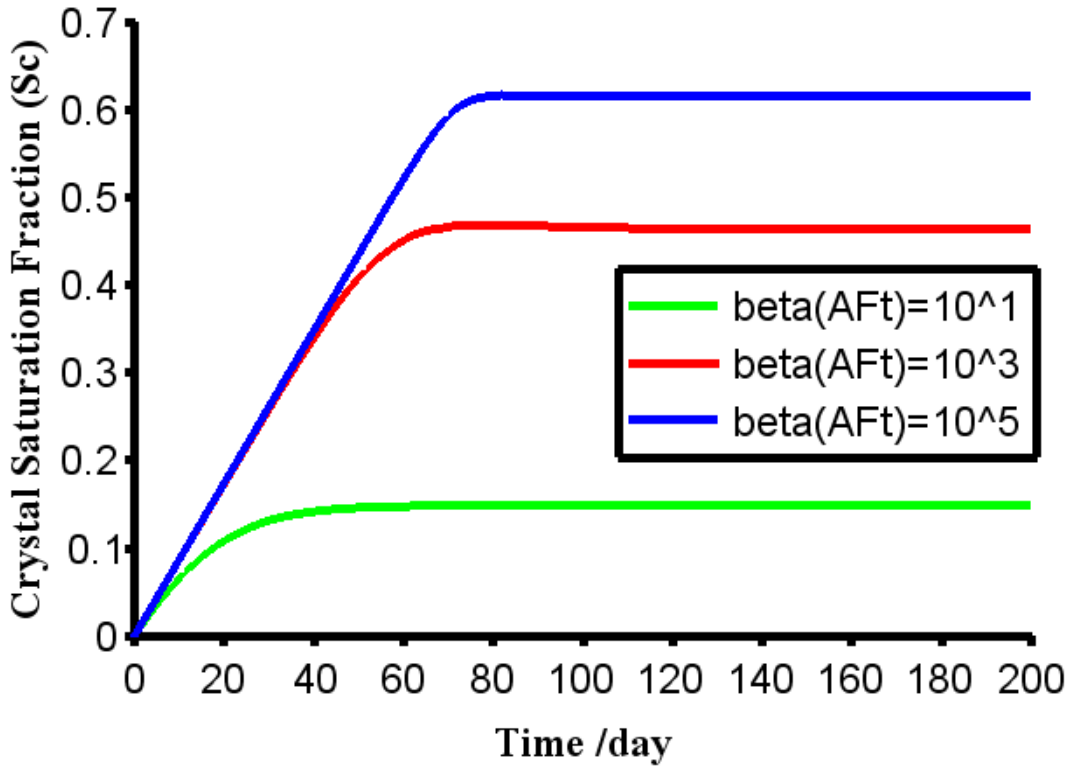


(a) in capillary pores $a = 10^{-7}$

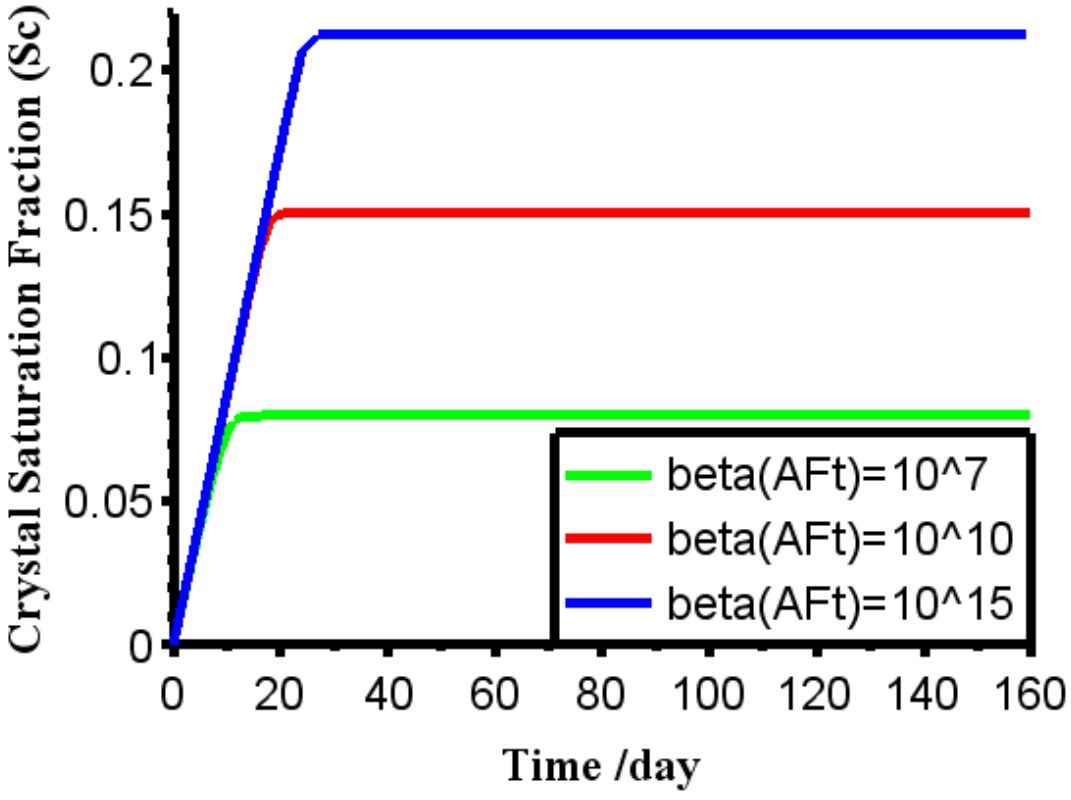


(b) in gel pores $a = 10^{-7}$

FIGURE 3 – Effect of the ettringite saturation index on the crystal saturation

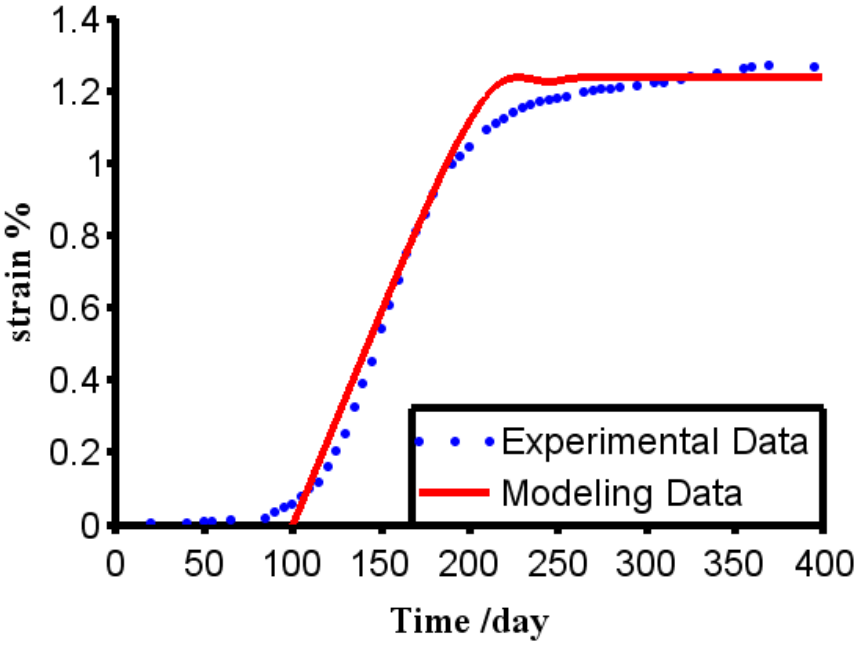


(a) Storage condition : 20°C
$a_1 = 1.25 \times 10^{-8}$, $\beta_{\text{AFt}} = 10^{8.2}$, $t_0 = 100day$, $K = 0.2GPa$, $b = 0.99$

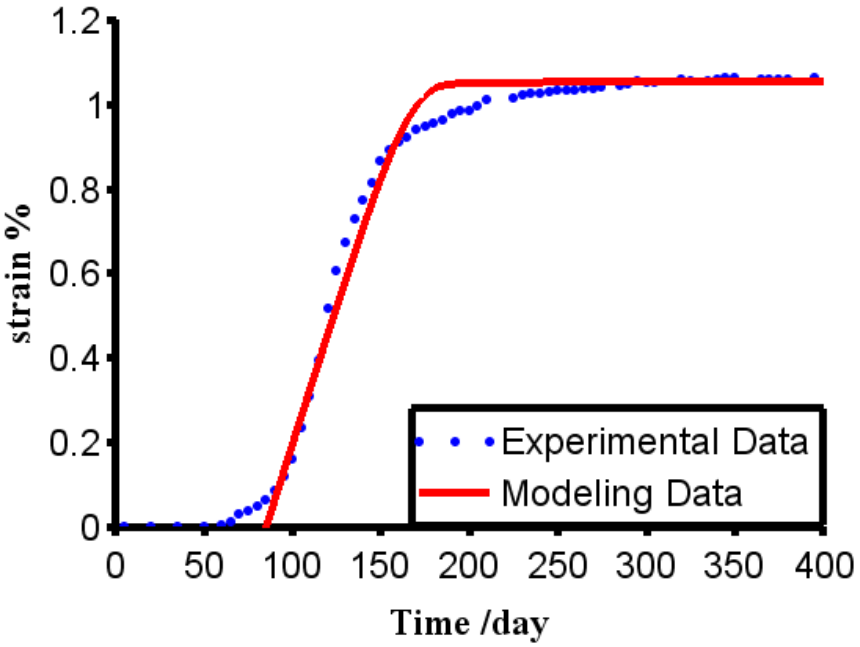


(b) Storage condition : 20°C 98 days and then 38°C
$a_2 = 1.5 \times 10^{-8}$, $\beta_{\text{AFt}} = 10^{7.75}$, $t_0 = 85day$, $K = 0.2GPa$, $b = 0.99$

FIGURE 4 – Calibration of parameters for DEF [1]

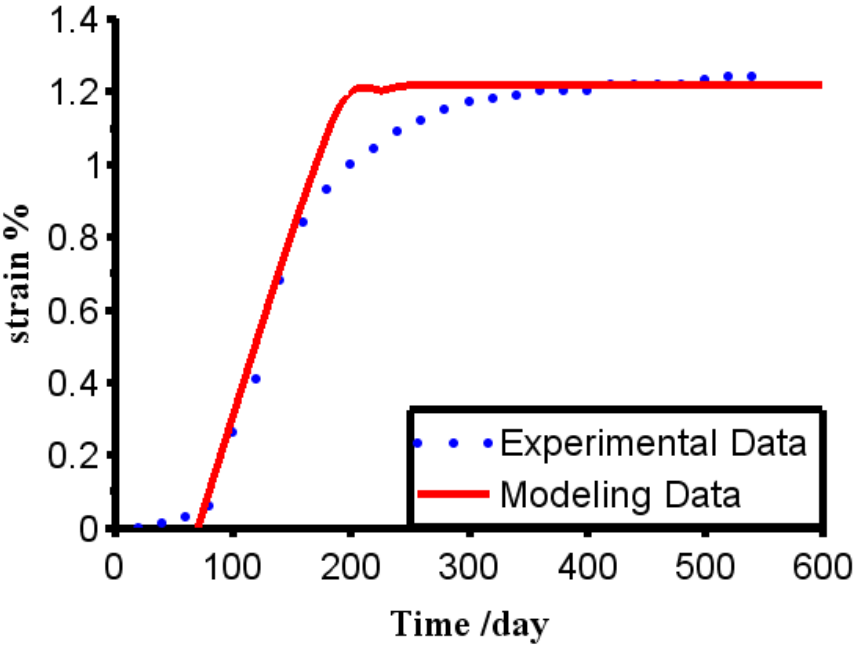


(a) Storage of 100% RH :
$a_1 = 1.1 \times 10^{-8}$, $\beta_{\text{AFt}} = 10^{8.15}$, $t_0 = 70day$, $K = 0.2GPa$, $b = 1$

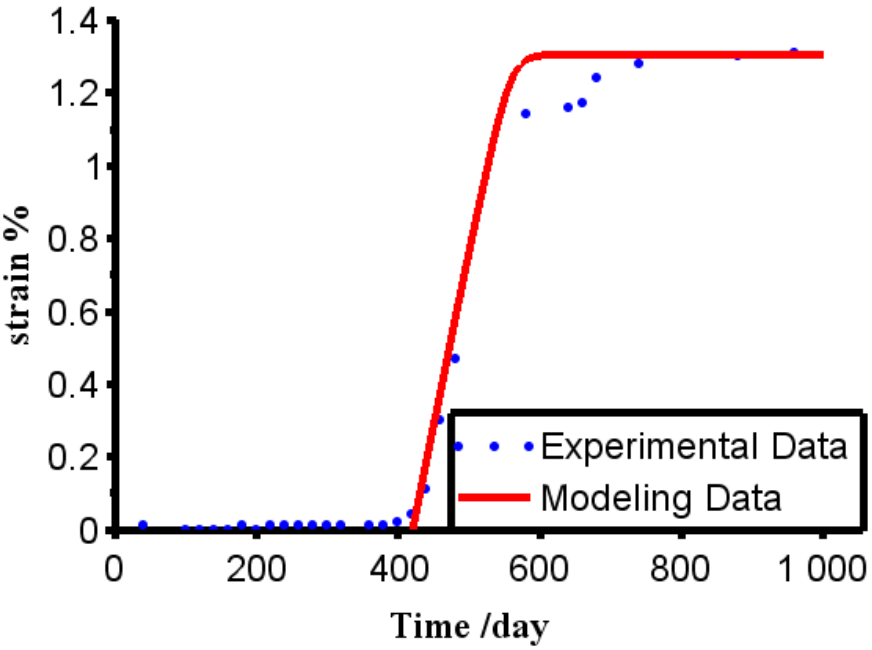


(b) Storage of 91% RH and immersed in water from the 334th day :
$a_2 = 1 \times 10^{-8}$, $\beta_{\text{AFt}} = 10^{8.36}$, $t_0 = 420day$, $K = 0.2GPa$, $b = 1$

FIGURE 5 – Calibration of parameters for DEF [8]

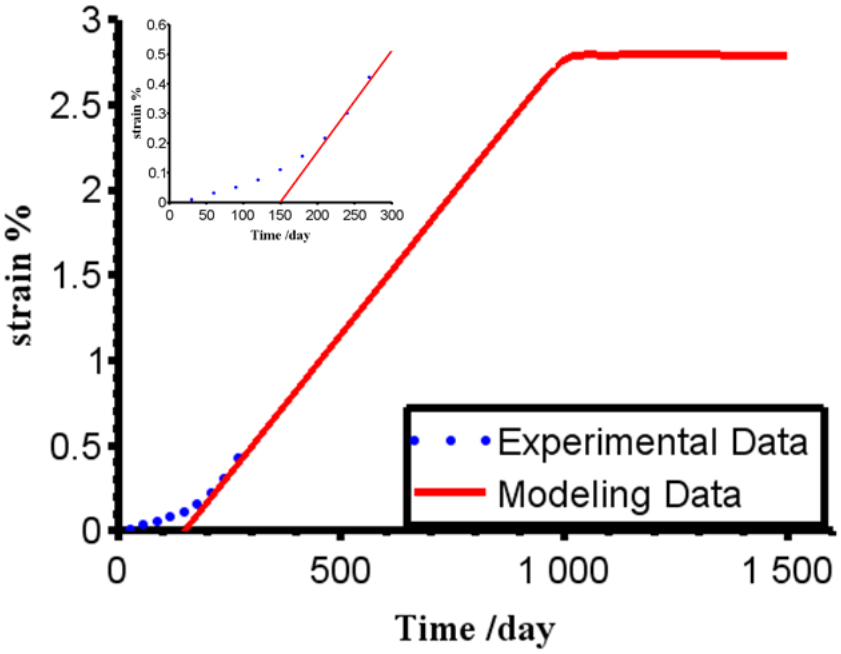


(a) $C_3A$ content of cement : 8.8%
$a_1 = 1 \times 10^{-8}$, $\beta_{\text{AFt}} = 10^{8.8}$,$t_0 = 150day$, $K = 0.6GPa$, $b = 1$

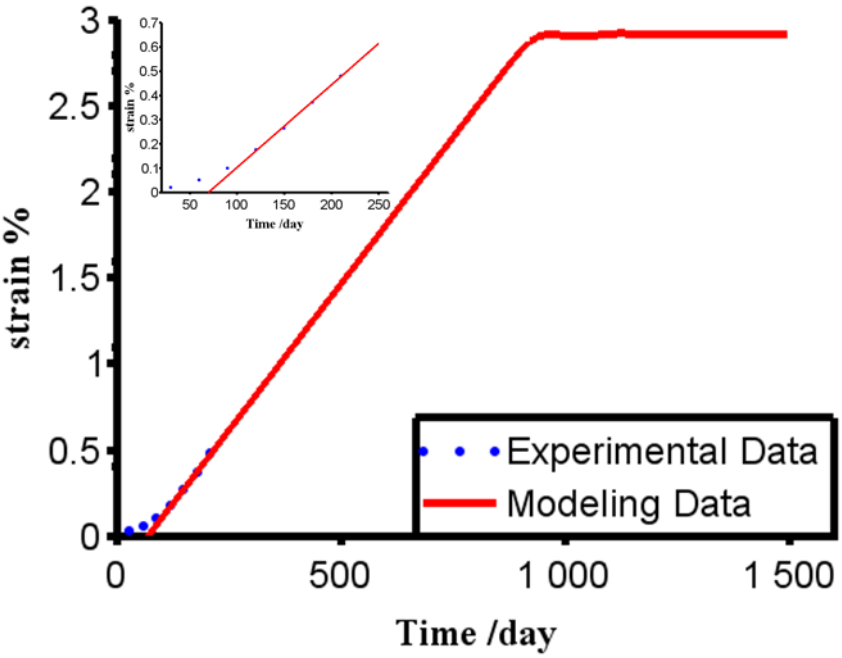


(b) $C_3A$ content of cement : 12%
$a_2 = 1 \times 10^{-8}$, $\beta_{\text{AFt}} = 10^{8.8}$,$t_0 = 70day$, $K = 0.6GPa$, $b = 1$

FIGURE 6 – Calibration of parameters for ESA [9]

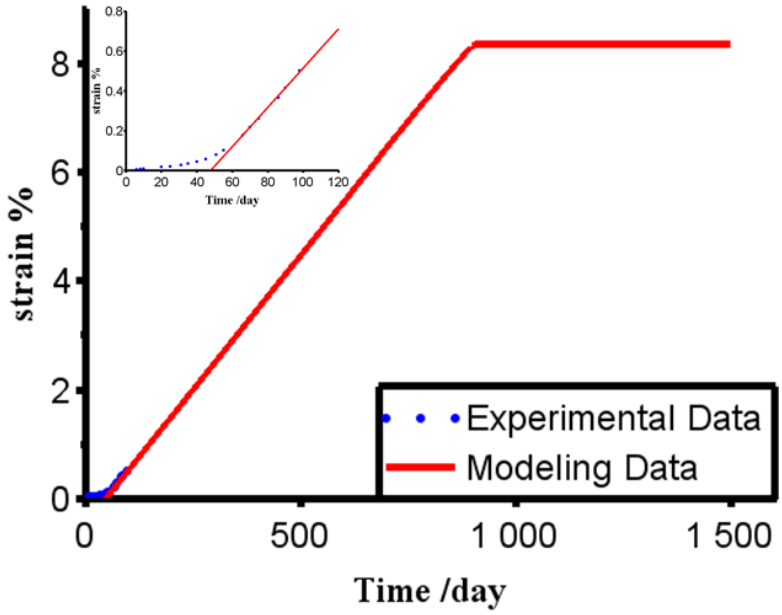


(a) pH not controlled solution :
$a_1 = 1 \times 10^{-8}$, $\beta_{\text{AFt}} = 10^{8.5}$,$t_0 = 48day$, $K = 0.2GPa$, $b = 1$

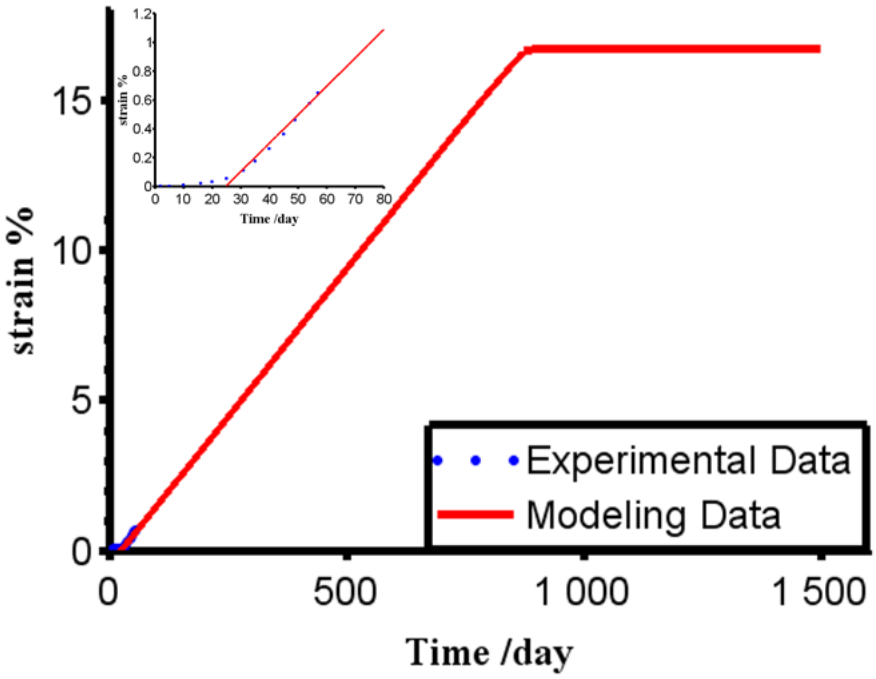


(b) pH controlled solution at 6 :
$a_2 = 1 \times 10^{-8}$, $\beta_{\text{AFt}} = 10^{8.5}$,$t_0 = 25day$, $K = 0.1GPa$, $b = 1$

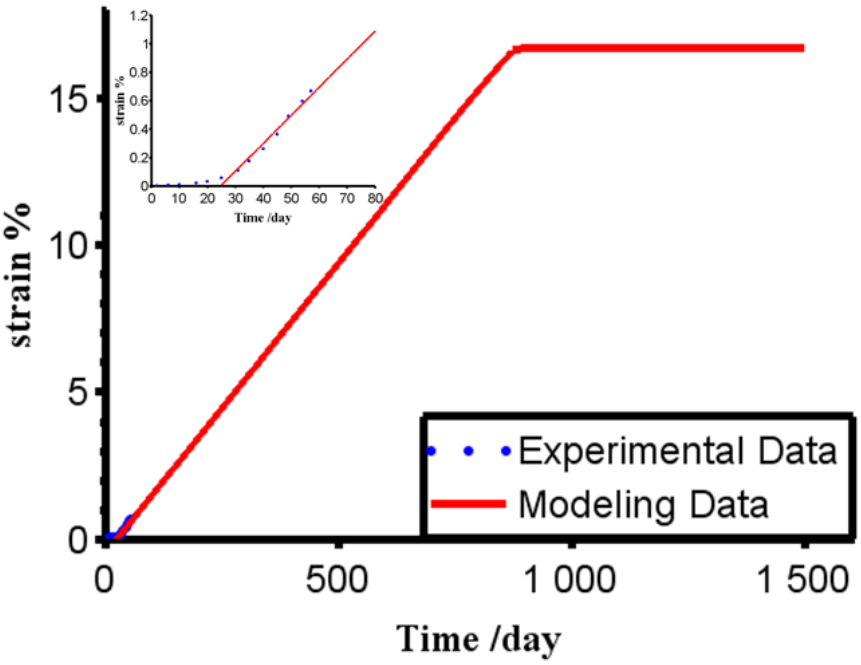


(a) pH controlled solution at 10 :
$a_3 = 1 \times 10^{-8}$, $\beta_{\text{AFt}} = 10^{8.5}$,$t_0 = 25day$, $K = 0.1GPa$, $b = 1$

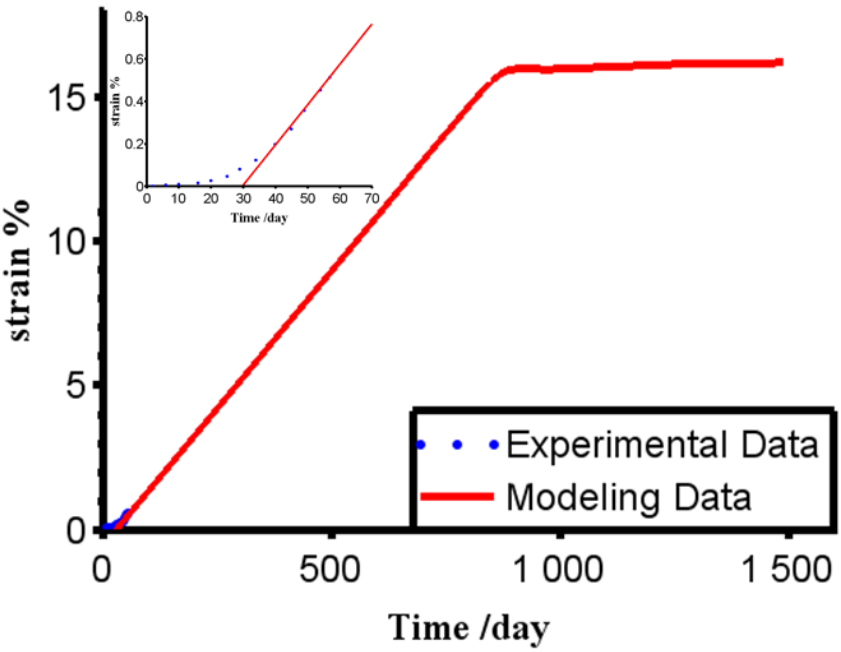


(b) pH controlled solution at 11.5 :
$a_4 = 1 \times 10^{-8}$, $\beta_{\text{AFt}} = 10^{8.2}$,$t_0 = 30day$, $K = 0.1GPa$, $b = 1$

FIGURE 7 – Calibration of parameters for ESA [10]